

Spontaneous CP violating quark scattering from asymmetric $Z(3)$ interfaces in QGP

Abhishek Atreya,^{*} Partha Bagchi,[†] Arpan Das,[‡] and Ajit M. Srivastava[§]
Institute of Physics, Bhubaneswar, 751005, India

In this paper, we extend our earlier study of spontaneous CP violating scattering of quarks and anti-quarks from QCD $Z(3)$ domain walls for the situation when these walls have asymmetric profiles of the Polyakov loop order parameter $l(x)$. Dynamical quarks lead to explicit breaking of $Z(3)$ symmetry, which lifts the degeneracy of the $Z(3)$ vacua arising from spontaneous breaking of the $Z(3)$ symmetry in the quark-gluon plasma (QGP) phase. Resulting domain walls have asymmetric profile of $l(x)$ (under reflection $x \rightarrow -x$ for a domain wall centered at the origin). We calculate the background gauge field profile A_0 associated with this domain wall profile. Interestingly, even with the asymmetric $l(x)$ profile, quark-antiquark scattering from the corresponding gauge field configuration does not reflect this asymmetry. We show that the expected asymmetry in scattering arises when we include the effect of asymmetric profile of $l(x)$ on the effective mass of quarks and antiquarks and calculate resultant scattering. We discuss the effects of such asymmetric $Z(3)$ walls in generating quark and antiquark density fluctuations in cosmology, and in relativistic heavy-ion collisions e.g. event-by-event baryon fluctuations.

PACS numbers: 25.75.-q, 12.38.Mh, 11.27.+d

I. INTRODUCTION

Search for the quark-gluon plasma (QGP) phase of QCD in relativistic heavy-ion collision experiments (RHICE) has reached a mature stage with observations providing compelling evidence that QGP phase is created in these experiments. While a definitive conclusion about the discovery of QGP is still awaited, it is an appropriate stage to explore new effects and new structures in this exotic phase of QCD. This is particularly important due to its implications for the case of early universe as well as for the cores of dense astrophysical objects like neutron stars. One such new effect is the possibility of extended topological objects in the QGP phase which arise from spontaneous breaking of the center symmetry $Z(3)$ of the color $SU(3)$ group. The $Z(3)$ symmetry is broken spontaneously as the Polyakov loop, $l(x)$, which is an order parameter for the confinement-deconfinement phase transition for pure gauge theory, [1] assumes a non-zero value in the deconfined phase. The resulting domain walls, so called $Z(3)$ walls [2–4], are in some sense similar to the axionic domain walls in the universe. Interestingly, just like axionic cosmic strings, here also there are topological strings associated with the junctions of these $Z(3)$ walls [5]. The study of these defects becomes more relevant in the present era of relativistic heavy-ion collision experiments as the temperature and energy densities that are needed to form these defects is (hopefully) accessible in these accelerators. In fact, these defects are the only defects in a relativistic quantum field theory that can be probed in the present day laboratory conditions.

In earlier works, some of us have studied the formation and evolution of these topological objects in the initial transition to the QGP phase in the context of RHICE [6]. Various consequences of $Z(3)$ walls have been discussed in these works for RHICE arising from nontrivial scattering of quarks from $Z(3)$ walls. Implications of the existence of these walls in the early universe has also been discussed in [7] where it is shown that baryon inhomogeneities can arise from scattering of quarks from $Z(3)$ walls. Scattering of quarks/antiquarks was studied in [7] by modeling the dependence of effective quark mass on the magnitude of the Polyakov loop order parameter $l(x)$. Spatially varying profile of $l(x)$ leads to spatially varying effective mass, which behaves as potential in the Dirac equation for quarks/antiquarks leading to non-trivial scattering. As this effective mass (potential) is the same for quarks and antiquarks, resulting scattering is the same for both.

In [8] we followed a different method for studying the scattering of quarks/antiquarks from $Z(3)$ walls. We assume that the profile of $l(x)$ corresponds to a sort of condensate of the background gauge field A_0 (following the definition of the Polyakov loop order parameter). We calculate this profile of the background gauge field from the profile of $l(x)$. Such a gauge field configuration, when used in the Dirac equation, leads to a potential which is different for quark

^{*}Electronic address: atreya@iopb.res.in

[†]Electronic address: partha@iopb.res.in

[‡]Electronic address: arpan@iopb.res.in

[§]Electronic address: ajit@iopb.res.in

and antiquark, leading to spontaneous CP violation in the scattering of quarks and antiquarks from a given $Z(3)$ wall. This CP violation is spontaneous as it arises from a specific background configuration of the gauge field corresponding to a given $Z(3)$ wall. This was first discussed by Altes et al. [9, 10] who argued in the context of the universe, that due to the non-trivial background field configuration for the standard model gauge fields, the localization of quarks and antiquarks on the wall is different. Its possible effects on the electroweak baryogenesis via sphalerons was discussed in [9, 10]. This spontaneous CP violation for the case of QCD was also discussed in [11]. The CP violating effects discussed in above works were primarily qualitative, as the exact profiles of A_0 were not calculated. In [8], we use the profile of Polyakov loop $l(x)$ between different $Z(3)$ vacua (which was obtained by using specific effective potential for $l(x)$ as discussed in [12]) to obtain the full profile of the background gauge field A_0 . This background A_0 configuration acts as a potential for quarks and antiquarks causing non-trivial reflection of quarks from the wall. There we also showed that this spontaneous CP violation arising from the background A_0 configuration leads to different reflection coefficients for quarks and antiquarks. In a series of follow up works [13, 14], we studied the effect of this difference in the scattering of quarks and antiquarks from $Z(3)$ walls in the context of ongoing relativistic heavy-ion collision experiments and the early universe. In [13], we discussed a novel mechanism of J/ψ disintegration in the relativistic heavy ion collision experiments. We showed that the localized electric field in the CP violating $Z(3)$ domain wall in the QGP phase lead to disintegration of quarkonia. In [14], we studied the effect of this CP violation on baryon transport across the collapsing $Z(3)$ domain walls in the early universe. We showed that it can lead to formation of quark nuggets as well as antiquark nuggets by segregating baryons and antibaryons in different regions of the universe near QCD phase transition epoch. As quarks are concentrated in a given collapsing domain wall, similar amount of antiquarks get concentrated in another collapsing domain wall which has the CP conjugate configuration of A_0 corresponding to the interchange of the two $Z(3)$ vacua with respect to the first domain wall case. Thus, for a given size of collapsing domain walls, resulting nugget sizes are identical for quarks and antiquarks.

There have been some objections on the existence of $Z(3)$ walls, (and of the associated field A_0) in the Minkowski space. We refer to our earlier work [8] for a discussion on this aspect. In our above mentioned studies of CP violating scattering of quarks/antiquarks from $Z(3)$ walls we have neglected the effect of quarks. The existence of these $Z(3)$ walls becomes a non-trivial issue in the presence of quarks. It has been argued that $Z(3)$ symmetry loses its meaning in the presence of dynamical quarks [15, 16]. Another approach to this issue is to regard the effect of quarks in terms of the explicit breaking of $Z(3)$ symmetry [17–19]. This finds support in the recent lattice calculations of QCD with quarks [20], which suggest that there is a strong possibility of existence of these $Z(3)$ vacua at high temperature. Since the presence of quarks lifts the degeneracy of different $Z(3)$ vacua, the $Z(3)$ interfaces are no more solutions of time independent field equations as they move away from the region with the unique true vacuum. However, it is important to note that with quark effects (taken in terms of explicit symmetry breaking), the interfaces survive as non-trivial topological structures, even though they do not remain solutions of time independent equations of motion. As the resulting profile of $l(x)$ between the true vacuum and a metastable vacuum is no more symmetric, it raises interesting possibilities for the generation of quark and antiquark inhomogeneities as a network of collapsing domain walls is considered, with different walls interpolating between different sets of $Z(3)$ vacua. Situation is even more interesting as with explicit symmetry breaking certain closed domain walls with true vacuum inside (and with sufficiently larger size) may expand [21]. This can lead to concentration of quarks and antiquarks in a shell like structure, which can have important implications in cosmology (for large shells) and in RHICE where it may imply concentration of baryons or antibaryons near the surface of the QGP region. With these motivations, we extend our earlier study of [8] in this paper with incorporation of the effects of explicit symmetry breaking arising from dynamical quarks. We find that even though the profile of $l(x)$ is asymmetric in this case (under reflection $x \rightarrow -x$) quark-antiquark scattering from the gauge field configuration associated with it does not show any difference from the symmetric case when explicit $Z(3)$ symmetry breaking is absent. More precisely, the scattering of a quark from left on the wall is identical to the scattering of an antiquark from the right. We then include the effect of asymmetric profile of $l(x)$ on the effective mass of quarks and antiquarks and calculate resultant scattering. Due to asymmetric profile of $l(x)$ the resulting effective mass of quarks and antiquarks is different when considering scattering from the left or from the right. (Though it is the same for quark and antiquark.) This, combined with the CP violating scattering resulting from the background gauge field configuration associated with this $l(x)$, leads to left-right asymmetry in scattering of quarks (from left) and antiquarks (from right). This will lead to important differences in resulting concentrations of quarks and antiquarks in cosmology as well as in RHICE.

The paper is organized in the following manner. In section II we recall the basic physics of the origin of spontaneous CP violation due to the presence of $Z(3)$ interfaces and briefly introduce the effective potential for the Polyakov loop incorporating explicit breaking of $Z(3)$ symmetry. Calculation of the *asymmetric* profile of $l(x)$ for this case and its associated gauge field configuration is somewhat non-trivial and we discuss this in section III. In section IV we first discuss the scattering of quarks and antiquarks from this gauge field configuration and show that it leads to the same results for quark and antiquark concentrations as for the case without any explicit symmetry breaking. We then introduce $l(x)$ dependent effective mass for quarks and antiquarks and show that the resultant scattering is different

for quarks (from the left) and antiquarks (from the right). Section V presents discussion and conclusions where we discuss possible implications of these results for cosmology and for RHICE.

II. SPONTANEOUS CP VIOLATION FROM Z(3) WALLS

We briefly recall the basic physics of the origin of the spontaneous CP violation arising from $Z(3)$ walls. The source of this CP violation is a background condensate of the gauge field A_0 which we take to correspond to the profile of $l(x)$. This association is made following the definition of the Polyakov loop, [1, 22, 23]

$$L(x) = \frac{1}{N} \text{Tr} \left[\mathbf{P} \exp \left(ig \int_0^\beta A_0(\vec{x}, \tau) d\tau \right) \right], \quad (1)$$

where $A_0(\vec{x}, \tau) = A_0^a(\vec{x}, \tau) T^a$, ($a = 1, \dots, N$) are the gauge fields and T^a are the generators of $SU(N)$ in the fundamental representation. \mathbf{P} denotes the path ordering in the Euclidean time τ , and g is the gauge coupling. Under global $Z(N)$ symmetry transformation, the Polyakov Loop transforms as

$$L(x) \longrightarrow Z \times L(x), \quad \text{where } Z = e^{i\phi}, \quad (2)$$

with $\phi = 2\pi m/N$; $m = 0, 1, \dots, (N-1)$.

Thermal average of the Polyakov loop, $\langle L(x) \rangle$, (which we denote as $l(x)$) is related to the free energy of an infinitely heavy test quark in a pure gluonic medium ($l(x) \propto e^{-\beta F}$). In the confined phase, a test quark should have infinite energy implying that $l(x) = 0$. In the deconfined phase, a test quark will have finite energy implying non-zero value of $l(x)$. Thus $l(x)$ serves as an order parameter for the confinement-deconfinement transition. In view of Eq.(2), a non-zero value of $l(x)$ leads to spontaneous breaking of $Z(N)$ symmetry in the high temperature deconfined phase, while this symmetry is restored in the low temperature confined phase when $l(x) = 0$. For QCD, $N = 3$, hence confinement-deconfinement transition in QCD corresponds to spontaneous breaking of $Z(3)$ symmetry leading to $Z(3)$ domain walls (and associated QGP string, see ref.[5]).

We emphasize that, though certainly there are conceptual issues regarding the existence of these structures [15, 16], by no means their existence can be ruled out. In fact, amongst all models allowing for existence of topological extended structures (domain walls, strings etc. which have been proposed in various particle physics theories in the early universe), these $Z(3)$ domain walls (and the associated QGP string) are the most well motivated. Indeed, if these objects exist, these will be the only relativistic field theory topological solitons which are accessible in laboratory experiments. Their detection will not only provide deep insights in the non-trivial physics of the QGP phase, it will have very important implications for cosmology.

As we mentioned, we determined the background gauge field configuration A_0 from the profile of $l(x)$ for a specific domain wall which interpolates between two $Z(3)$ vacua without quark effects. For determining the profile of $l(x)$ interpolating between different $Z(3)$ vacua we used the specific effective potential for the Polyakov loop from ref. [12] with the Lagrangian density given by

$$L = \frac{N}{g^2} |\partial_\mu l|^2 T^2 - V(l). \quad (3)$$

Here $N = 3$ for QCD. T^2 is multiplied with the first term to give the correct dimensions to the kinetic term. The effective potential $V(l)$ for the Polyakov loop is given as

$$V(l) = \left(-\frac{b_2}{2} |l|^2 - \frac{b_3}{6} (l^3 + (l^*)^3) + \frac{1}{4} (|l|^2)^2 \right) b_4 T^4. \quad (4)$$

The coefficients b_2 , b_3 and b_4 are dimensionless quantities. These parameters are fitted in ref.[17–19] such that that the effective potential reproduces the thermodynamics of pure $SU(3)$ gauge theory on lattice [24, 25]. The coefficients are $b_2 = (1 - 1.11/x)(1 + 0.265/x)^2(1 + 0.300/x)^3 - 0.478$, (with $x = T/T_c$ and $T_c \sim 182$ MeV), $b_3 = 2.0$ and $b_4 = 0.6061 \times 47.5/16$. With these values, $l(x) \longrightarrow y = b_3/2 + \frac{1}{2} \times \sqrt{b_3^2 + 4b_2} (T = \infty)$ as $T \longrightarrow \infty$. Various quantities are then rescaled such that $l(x) \longrightarrow 1$ as $T \longrightarrow \infty$. The scaling are

$$l(x) \rightarrow \frac{l(x)}{y}, \quad b_2 \rightarrow \frac{b_2}{y^2}, \quad b_3 \rightarrow \frac{b_3}{y}, \quad b_4 \rightarrow b_4 y^4. \quad (5)$$

At low temperature where $l = 0$, the potential has only one minimum. For temperatures higher than T_c , the Polyakov loop develops a non vanishing vacuum expectation value l_0 , and the cubic term above leads to $Z(3)$ degenerate vacua.

The $l(x)$ profile is calculated by energy minimization, see ref.[5] for details. From the $l(x)$ profile, the A_0 profile is calculated by inverting Eq. (1). For various conceptual issues regarding this calculation we refer to our earlier work [8]. To address the issue of uncertainties in the determination of the A_0 profile depending on the choice of the specific form of the effective potential, we had repeated this calculation of A_0 profile, in ref.[8], for another choice of effective potential of the Polyakov loop as provided by Fukushima [26]. It was found that even though the two effective potentials (in refs.[12] and [26]) are of qualitatively different shapes, the resulting wall profile and A_0 profile were very similar. This gives us confidence that our conclusions arising from the calculations of scattering of quarks and antiquarks from $Z(3)$ walls are not crucially dependent on the specific choice of the effective potential.

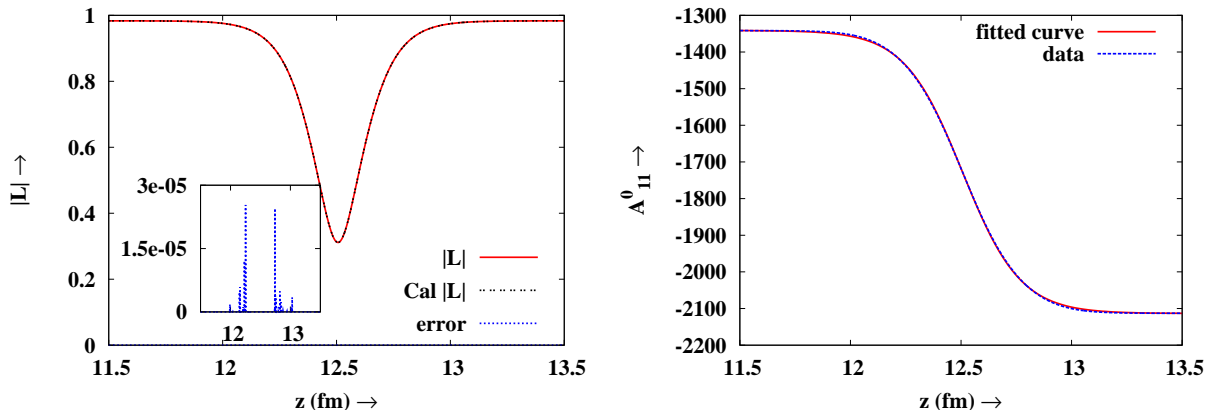


FIG. 1: Plot of $|l(x)|$ obtained from energy minimization for $b_1 = 0.0$ and $T = 400$ MeV. The corresponding A_0 configuration is on right. A_0 profile fits well with a tanh function.

We now include the effects of dynamical quarks leading to explicit breaking of $Z(3)$ symmetry. For this, we will follow the approach where the explicit breaking of the $Z(3)$ symmetry is represented in the effective potential by inclusion of a linear term in l [17–19, 27]. The above potential $V(l)$ with the linear term becomes,

$$V(l) = \left(-\frac{b_1}{2}(l + l^*) - \frac{b_2}{2}|l|^2 - \frac{b_3}{6}(l^3 + l^{*3}) + \frac{1}{4}(|l|^2)^2 \right) b_4 T^4 \quad (6)$$

Here coefficient b_1 measures the strength of explicit symmetry breaking. (In view of Eq.(5), b_1 is scaled as $b_1 \rightarrow b_1/y^3$.) A discussion on various values that b_1 can have is given in [27]. A non-zero value of b_1 lifts the degeneracy between the three $Z(3)$ vacua. Vacua corresponding to $\theta = 2\pi/3$ ($l = z$) and $\theta = 4\pi/3$ ($l = z^2$) remain degenerate, while the true vacuum with a lower energy corresponds to $l = 1$ ($\theta = 0$). Thus, $l = z$ and $l = z^2$ vacua become metastable. The value of b_1 can be related to the estimates of explicit $Z(3)$ symmetry breaking arising from quark effects which have been discussed in the literature. In the high temperature limit, the estimate of the difference in the potential energies of the $l = z$ vacuum, and the $l = 1$ vacuum, ΔV , is given in ref. [28] as,

$$\Delta V \sim \frac{2}{3}\pi^2 T^4 \frac{N_l}{N^3} (N^2 - 2) \quad (7)$$

where N_l is the number of massless quarks. If we take $N_l = 2$ then $\Delta V \simeq 3T^4$. For $T = 400$ MeV, this value of ΔV is obtained if we take the value of $b_1 = 0.645$. For temperatures of order T_c , it is not clear what should be the appropriate value of b_1 . It is entirely possible, that b_1 may be very small near T_c . (Possible reasons for taking very small values of b_1 are discussed in detail in ref. [21].) In view of these uncertainties in the magnitude of explicit symmetry breaking for temperatures near T_c , we will consider a range of values of b_1 including very small value of $b_1 = 0.03$, and determine the profile of $l(x)$ and the associated A_0 profile for these values of b_1 .

III. PROFILES OF $l(x)$ AND ASSOCIATED GAUGE FIELD CONFIGURATION WITH EXPLICIT SYMMETRY BREAKING

The explicit symmetry breaking arising from quark effects will have important effects on the structure of $Z(3)$ walls. For non-degenerate vacua, even planar $Z(3)$ interfaces do not remain static, and move away from the region

with the unique true vacuum. Thus, while for the degenerate vacua case every closed domain wall collapses, for the non-degenerate case this is not true any more. A closed wall enclosing the true vacuum may expand if it is large enough so that the surface energy contribution does not dominate.

The absence of time independent solutions of the field equations for $Z(3)$ walls leads to complications in the implementation of the techniques of ref. [5] for determination of $l(x)$ profile for the domain wall which were based on the algorithm of energy minimization. In ref.[5], correct $l(x)$ profile was obtained from an initial trial profile by fluctuating the value of $l(x)$ at each lattice point and determining the acceptable fluctuation which lowers the energy (with suitable overshoot criterion etc. as described in detail in ref.[5]). For the case without explicit symmetry breaking, a trial initial configuration of $l(x)$ with appropriate fixed boundary conditions (corresponding to the two $Z(3)$ vacua under consideration) yielded correct profile of $l(x)$ for the wall within relatively few iterations. However, with explicit symmetry breaking, this simple procedure fails as energy can always be lowered by shifting the wall towards to metastable vacua (thus expanding the region with true vacuum).

From the computational point of view, one of the major change due to the inclusion of b_1 term is the the scaling. Without b_1 all the vacua are degenerate, so $|l(x)| \rightarrow 1$ in all the vacua. However, that is not the case with the potential given by Eq. (6). This leads to the b_1 dependence of the scaling. We normalize the potential in such a manner that $|l(x)| \rightarrow 1$ in the true vacuum. As we mentioned above, the energy splitting between vacua itself amounts to a pressure difference between the two vacua. Thus the program tries to minimize the energy by moving the domain wall in one direction till it goes completely out of the lattice, in the process it changes the boundary values too if they are not held fixed. If we fix the boundary value in the far left and far right region of lattice, the program minimizes the energy by not only moving the profile in the intermediate region but also by re-adjusting the values of $|l(x)|$ on the two sides. The effect is most pronounced for the large b_1 . This statement becomes clearer if we look at the Fig. 2. It shows the initial and the final profile of $l(x)$ between $l = 1$ and $l = z$ vacua for $b_1 = 0.645$ at $T = 400$ MeV. The asymmetry is pretty clear in the boundary conditions of the initial trial configuration itself. Note the central region in the final configuration (solid curve). There is a sharp variation of $|l(x)|$ in a small region and on either side of it the $|l(x)|$ values are same (but different from actual boundary values) leading to a stable configuration in the middle. Since the domain wall is characterized by the sharp variation of the field in a small spatial region, we fit the profile such that it meets the correct boundary values while keeping the variation as given by the energy minimization program. This is shown by the dotted curve in the left figure. Though this procedure of *smoothing* the domain wall profile near its edges is somewhat ad hoc, it will not affect our results much as the scattering of quarks and antiquarks are primarily decided by the height and width of the sharply varying profile of $l(x)$. On comparing with Fig. (1) (for $b_1 = 0$ case), we note that explicit breaking of $Z(3)$ symmetry leads to asymmetric profiles of $l(x)$. This immediately suggests that there will be a difference between the scattering of a quark coming from the right and the scattering of the one coming from left.

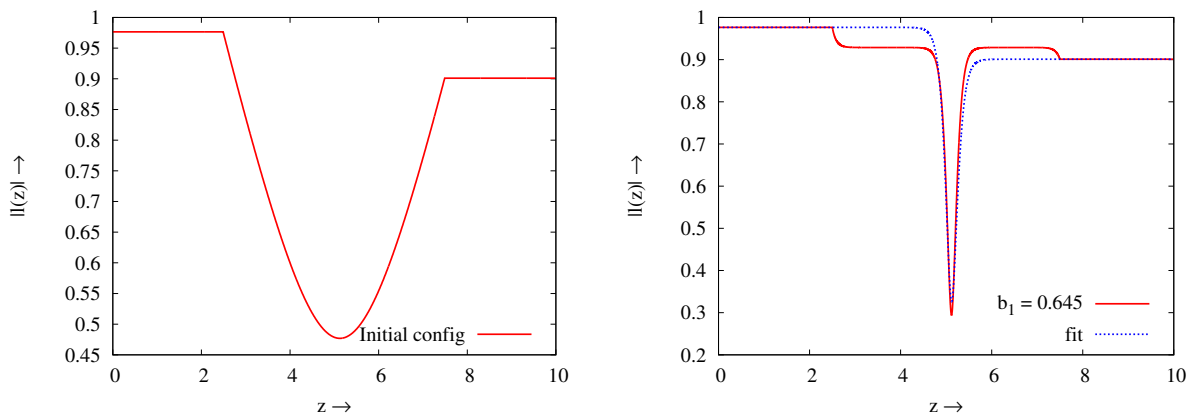


FIG. 2: Plot of $|l(x)|$ obtained from energy minimization for $b_1 = 0.645$ (solid curve). On the left is the initial trial configuration. The final configuration is on right.

The A_0 profile corresponding to the $l(x)$ profile was calculated in our earlier paper [8], where we also discussed various conceptual issues related to the ambiguities in the extraction of a colored quantity A_0 from color singlet $l(x)$. We choose Polyakov gauge (diagonal gauge) for A_0 :

$$A_0 = \frac{2\pi T}{g} (a\lambda_3 + b\lambda_8), \quad (8)$$

where, g is the coupling constant and T is the temperature, while λ_3 and λ_8 are the diagonal Gell-Mann matrices. The A_0 profile was obtained from $l(x)$ profile (Fig. 2) by inverting Eq.(1). For details, see ref. [8]. We have carried out this calculation for the profiles of $l(x)$ obtained from the energy minimization program for $b_1 \neq 0$ (Fig. (2)). The calculated a, b were then used to calculate A_0 using Eq. (8). The A_0 profile thus obtained is reasonably well fitted to the function $A_0(x) = p \tanh(qx + r) + s$ using gnuplot. The calculated A_0 profile and fitted A_0 profile are plotted in figure (3).

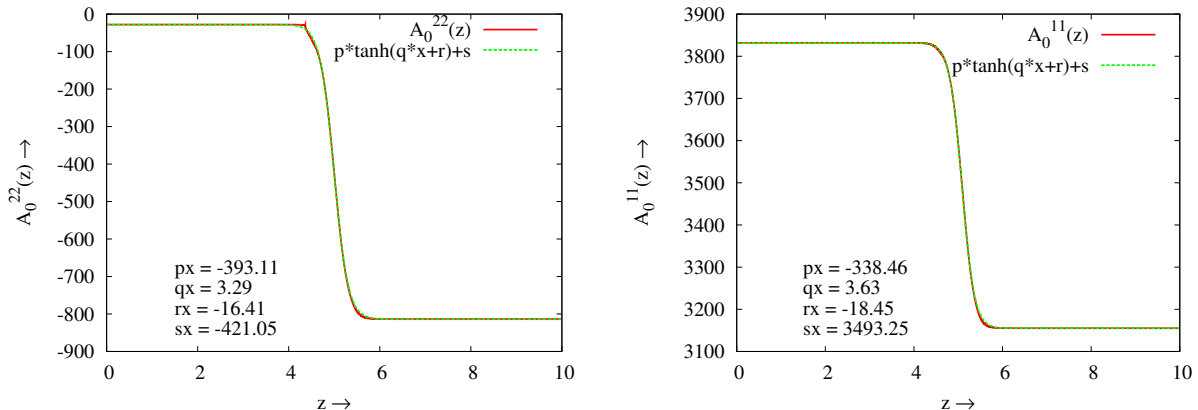


FIG. 3: Plot of calculated A_0 and the fitted profile ($A_0(x) = p \tanh(qx + r) + s$) for $b_1 = 0.03$ and 0.645 .

We note that the fit to tanh profile is almost perfect just as was the case for $b_1 = 0$ case in Fig. 1. We thus conclude that the scattering of a quark coming from left with such an A_0 profile (in the Dirac equation) will be the same as the scattering of an antiquark coming from right (with same kinetic energy). Thus a collapsing domain wall with $l = 1$ inside and $l = z$ outside will give same reflection coefficients (hence resulting concentration) for quarks inside as a collapsing domain wall with $l = z$ inside and $l = 1$ outside will give for antiquarks (assuming zero baryon chemical potential). This is interesting in view of the asymmetric profiles of $l(x)$ in Fig. 2 for $b_1 \neq 0$ cases. Though still there will be important differences from the $b_1 = 0$ case as now a sufficiently large closed domain wall with true vacuum ($l = 1$) inside will expand instead of collapsing, leading to concentration of quarks or antiquarks in a shell like region. We will discuss these possibilities later in section V.

It may also be noted that we have shown A_0^{11} for $b_1 = 0.645$ and A_0^{22} for $b_1 = 0.03$. This is for the reason that both the profiles are similar in the shape and size. It has to do with the choice of initial (a, b) values while calculating A_0 . This essentially means that we should compare the reflection of red quark in $b_1 = 0.645$ case with the reflection of green quark in $b_1 = 0.03$ case. One may use hit and trial method to find a specific choice of (a, b) in the case of $b_1 = 0.03$ such that A_0^{11} obtained has the same spatial variation as the one for $b_1 = 0.645$. We refer to ref. [8] for further details on this issue of initial conditions.

As we mentioned, it is interesting to note that asymmetry of $l(x)$ is not reflected in the background gauge configuration. The effect of non-zero b_1 is reflected in the A_0 profile not in terms of the change in shape but in terms of the height of the potential getting reduced. For $b_1 = 0.645$, the height of A_0 is almost 100 MeV less than the height of A_0 in $b_1 = 0.03$ case. However, this decrease in the height will not give any asymmetry in the reflection of quarks and anti-quarks from the A_0 , neither will it change the amount of reflection in a drastic fashion. We will now consider another possibility which allows for asymmetry in concentration of quarks and antiquarks for the $b_1 \neq 0$ case.

For this we recall the discussion of quark/antiquark scattering due to l dependent effective mass, as discussed in ref.[7]. The basic idea proposed in ref.[7] was that as $l(x)$ is the order parameter for the quark-hadron transition, physical properties such as effective mass of the quarks should be determined in terms of $l(x)$. This also looks natural from the expected correlation between the chiral condensate and the Polyakov loop. Lattice results indicate that the chiral phase transition and the deconfinement phase transition may be coupled, i.e as the Polyakov loop becomes non zero across T_c , the chiral order parameter attains a vanishingly small value. Thus, if there is spatial variation in the value of $l(x)$ in the QGP phase then effective mass of the quark traversing that region should also vary (say, due to spatially varying chiral condensate). For regions where $l(x) = 0$, quarks should acquire constituent mass as appropriate for the confining phase. To model the dependence of effective quark mass on $l(x)$ we could use the color dielectric model of ref.[29] identifying $l(x)$ with the color dielectric field χ in ref.[29]. Effective mass of the quark was modeled in [29] to be inversely proportional to χ . This leads to divergent quark mass in the confining phase consistent with the notion of confinement. However, we know that the divergence of quark energy in the confining phase should

be a volume divergence (effectively the length of string connecting the quark to the boundary of the volume). $1/l(x)$ dependence will not have this feature, hence we do not follow this choice. For the sake of simplicity, and for order of magnitude estimates at this stage, we will model the quark mass dependence on $l(x)$ in the following manner.

$$m(x) = m_q + m_0(l_0 - |l(x)|) \quad (9)$$

Here $l(x)$ represents the profile of the $Z(3)$ domain wall, and l_0 is the vacuum value of $|l(x)|$ (for the true vacuum) appropriate for the temperature under consideration. m_q is the current quark mass of the quark as appropriate for the QGP phase with $|l(x)| = l_0$, with $m_u \simeq m_d = 10$ MeV and $m_s \simeq 140$ MeV. m_0 characterizes the constituent mass contribution for the quark. We will take $m_0 = 300$ MeV. Note that here $m(x)$ remains finite even in the confining phase with $l(x) = 0$. As mentioned above, this is reasonable since we are dealing with a situation where $l(x)$ differs from l_0 only in a region of thickness of order $1fm$ (thickness of domain wall).

The space dependent part of $m(x)$ in Eq.(9) is taken as a potential term in the Dirac equation for the propagation of quarks and antiquarks. As we see from Fig.(1), $l(x)$ varies across a $Z(3)$ interface, acquiring small magnitude in the center of the wall. A quark passing through this interface, therefore, experiences a nonzero potential barrier leading to non-zero reflection coefficient for the quark. Important thing here is that due to asymmetric profile of l (Fig.(2)), the effective mass of quarks/antiquarks will have different values on the two sides of the domain wall. This effect, when combined with the scattering from the background A_0 configuration, will lead to asymmetry in the scattering of quarks from one side and that of antiquarks from the other side of the domain wall.

One may be concerned here whether combining the scattering from A_0 configuration with the scattering due to l dependent effective mass amounts to double counting in the sense that both effects originate from the same $l(x)$ profile. For this we note that there are indeed two different effects at play here due to the existence of $Z(3)$ walls. First effect arises from the existence of three different phases of QGP characterized by spontaneous breaking of $Z(3)$ symmetry. In the absence of explicit symmetry breaking one will expect that physics should be identical for these three phases. Thus, even l dependent effective mass of quarks should have the same value in these three phases, as indeed is the case from Eq.(9) due to same value of $|l|$ in the three $Z(3)$ phases. However, with explicit symmetry breaking, there is no physical argument to say that physics should be the same for the three $Z(3)$ vacua, as the two vacua ($l = z$ and $l = z^2$) become metastable. As $|l|$ in these two vacua has smaller magnitude, effective mass of quarks may actually be larger in these two phases of QGP. As explained for Eq.(9), we can think of this $|l|$ dependent mass in terms of chiral condensate whose value will depend on $l(x)$. (We mention that $l(x)$ dependent quark mass by itself is a non-trivial implication of our proposal and it will have many other interesting implications on propagation of quarks/antiquarks in QGP in the presence of these $Z(3)$ domains.) Next we come to the presence of background gauge field. This arises from spatial variation of $l(x)$ leading to color electric field from which quarks and antiquarks scatter in different manner. This color electric field is entirely localized at the boundary of $Z(3)$ domains (where $l(x)$ has spatial variation), and vanishes in the interiors of the $Z(3)$ domains. It couples differently to quarks/antiquarks of different color charges. Hence, this effect is entirely different from the effect of effective mass which has different values in the interiors of the two domains, irrespective of the color charges of quarks and antiquarks (even though for the scattering purposes, both effects lead to non-trivial potential at the location of the $Z(3)$ wall).

IV. REFLECTION AND TRANSMISSION COEFFICIENTS WITH EXPLICIT SYMMETRY BREAKING

We now calculate the reflection and transmission coefficient for quarks and antiquarks subject to the above two effects. One is CP violating, arising from the background gauge field A_0 (Eq.(8)), and the other is CP preserving, arising from the space dependent effective mass of quarks/antiquarks (Eq.(9)). We recall the steps for calculation from [8]. To calculate the reflection and transmission coefficient, we need the solutions of Dirac equation in the Minkowski space but the A_0 profile is calculated in Euclidean space. We start with the Dirac equation in the Euclidean space, with the spatial dependence of A_0 calculated from $Z(3)$ wall profile as mentioned above, and with space dependent mass term as given in Eq.(9).

$$[\gamma_e^0 \partial_0 \delta^{jk} - g\gamma_e^0 A_0^{jk}(z) + (i\gamma_e^3 \partial_3 + m(x))\delta^{jk}] \psi_k = 0, \quad (10)$$

where $\gamma_e^0 \equiv i\gamma^0$ and $\gamma_e^3 \equiv \gamma^3$ are the Euclidean Dirac matrices. ∂_0 denotes $\partial/\partial\tau$ with $\tau = it$ being the Euclidean time. j, k denote color indices. $m(x)$ is the effective mass as given in Eq.(9). We now analytically continue the Eq. (10) to the Minkowski space to get

$$[i\gamma^0 \partial_0 \delta^{jk} + g\gamma^0 A_0^{jk}(z) + (i\gamma^3 \partial_3 + m(x))\delta^{jk}] \psi_k = 0. \quad (11)$$

where now ∂_0 denotes $\partial/\partial t$ in the Minkowski space.

Eq.(11) is used to calculate the reflection and transmission coefficients. For a general smooth potential we followed a numerical approach given by Kalotas and Lee [30]. They have discussed a numerical technique to solve Schrödinger equation with potentials having arbitrary smooth space dependence. We applied this technique of ref.[30] for solving the Dirac equation (see, ref.[8] for details).

The results for different quarks and anti-quarks (with $E = 3.0$ GeV taken as example for each case) are given in table I. As we mentioned, the important quantity for us is to calculate the reflection coefficient of (say) quarks coming from the left of the wall and compare it with the reflection coefficient of antiquarks (with the same kinetic energy) coming from the right of the wall. Any (possible) difference in these two reflection coefficients directly relates to the expected concentration of quarks and antiquarks by a domain wall of one kind and its opposite wall (interpolating between the two $Z(3)$ vacua in reverse order). Table I shows clear difference in these two reflection coefficients.

	$b_1 = 0.03$	0.126	0.645
Left R_q	1.65437×10^{-6}	4.40706×10^{-6}	1.43314×10^{-10}
Right R_q	0.00003366	0.0141752	0.00394808
Left R_{aq}	2.25671×10^{-6}	1.85367×10^{-7}	2.07835×10^{-7}
Right R_{aq}	0.000376883	0.0820803	0.073885

TABLE I: Table for the reflection coefficients for various quarks and antiquarks for smooth profiles of A_0 and $m(x)$.

V. DISCUSSION

In this work we have extended our earlier studies of CP violating scattering of quarks/antiquarks from $Z(3)$ walls [8, 13, 14], by including the effects of explicit breaking of $Z(3)$ symmetry which is expected to arise due to dynamical quarks. The resulting profile of $l(x)$ between the true vacuum and a metastable vacuum is no more symmetric in this case which leads to new effects. We study scattering of quarks and antiquarks from the background A_0 field associated with the profile of $l(x)$ while also incorporating the effect of spatially varying effective mass of quarks and antiquarks in the respective $Z(3)$ domains. The combined effect of the scattering shows interesting behavior leading to left-right asymmetry in scattering of quarks (from left) and antiquarks (from right). This will lead to important differences in resulting concentrations of quarks and antiquarks in cosmology as well as in RHICE. For example, in the early universe, a network of domain walls will arise with varying sizes and interpolating between different $Z(3)$ vacua. For all domain walls of a given size interpolating between given two vacua in a given order, there will be roughly same number of walls with similar size but interpolating between the same two $Z(3)$ vacua in the reverse order. (Though explicit symmetry breaking may also produce difference between formation of such walls, introducing further richness in the effects of explicit symmetry breaking). In the absence of explicit symmetry breaking, if first type of walls give certain concentration of (say) quarks, then the other set of walls will give similar concentration of antiquarks. This is, however, not the case when explicit symmetry breaking effects are incorporated. In view of results from table I, the two sets of walls will lead to very different concentrations of quarks and antiquarks (especially if the value of b_1 is large). Though for each domain wall (say interpolating between $l = 1$ and $l = z$, there is always the *conjugate* wall (interpolating between $l = 1$ and $l = z^2$) which will lead to same scattering between quarks and antiquarks. Final effect of our results will then appear as two different magnitudes for the concentrations of quarks and antiquarks, even if one takes all domain walls of the same size. This is very different from the case without explicit symmetry breaking where domain walls of same size will lead to quark and antiquark inhomogeneities of same magnitude (for same kinetic energies of quarks and antiquarks). This difference will be particularly dramatic for RHICE where number of domain walls is of order one for each event [6]. Thus even for same type of events, one may get very different concentration of baryons or antibaryons in different events leading to very large event-by-event fluctuations.

Situation is even more interesting when we consider the effect that with explicit symmetry breaking certain closed domain walls may expand, those with true vacuum inside (and with sufficiently larger size so that volume energy difference dominates over the surface energy contribution [21]). This can lead to concentration of quarks and antiquarks in a shell like structure. For cosmology very large expanding domain walls may trap shells of baryons/antibaryons if enclosed by a collapsing *antiwall* configuration. Such shells can form in RHICE also and will have important observations signatures.

VI. ACKNOWLEDGMENTS

We are extremely thankful to Shreyash Shankar Dave, Sanatan Digal, and Saumia P.S. for fruitful discussions.

-
- [1] A. M. Polyakov, Phys. Lett. **B72**, 477 (1978).
 - [2] T. Bhattacharya, A. Gocksch, C. Korthals Altes, and R. D. Pisarski, Nucl. Phys. **B383**, 497 (1992).
 - [3] S. T. West and J. F. Wheeler, Nucl. Phys. **B486**, 261 (1997)
 - [4] J. Boorstein and D. Kutasov, Phys. Rev. **D51**, 7111 (1995)
 - [5] B. Layek, A. P. Mishra, and A. M. Srivastava, Phys. Rev. **D71**, 074015 (2005)
 - [6] U. S. Gupta, R. K. Mohapatra, A. M. Srivastava, and V. K. Tiwari, Phys. Rev. **D82**, 074020 (2010)
 - [7] B. Layek, A. P. Mishra, A. M. Srivastava, and V. K. Tiwari, Phys. Rev. **D73**, 103514 (2006)
 - [8] A. Atreya, A. M. Srivastava, and A. Sarkar, Phys.Rev. **D85**, 014009 (2012), 1111.3027.
 - [9] C. P. Korthals Altes, K.-M. Lee, and R. D. Pisarski, Phys.Rev.Lett. **73**, 1754 (1994)
 - [10] C. P. Korthals Altes and N. J. Watson, Phys. Rev. Lett. **75**, 2799 (1995),
 - [11] C. P. Korthals Altes (1992), in *Dallas 1992, Proceedings, High energy physics, vol. 2* 1443-1447.
 - [12] R. D. Pisarski, Phys. Rev. **D62**, 111501 (2000)
 - [13] A. Atreya, P. Bagchi, and A. M. Srivastava (2014), arXiv:1404.5697.
 - [14] A. Atreya, A. Sarkar, and A. M. Srivastava (2014), arXiv:1405.6492.
 - [15] A. V. Smilga, Ann. Phys. **234**, 1 (1994).
 - [16] V. M. Belyaev, I. I. Kogan, G. W. Semenoff, and N. Weiss, Phys. Lett. **B277**, 331 (1992).
 - [17] A. Dumitru and R. D. Pisarski, Phys. Lett. **B504**, 282 (2001)
 - [18] A. Dumitru and R. D. Pisarski, Nucl. Phys. **A698**, 444 (2002),
 - [19] A. Dumitru and R. D. Pisarski, Phys. Rev. **D66**, 096003 (2002),
 - [20] M. Deka, S. Digal, and A. P. Mishra (2010)
 - [21] U. S. Gupta, R. K. Mohapatra, A. M. Srivastava, and V. K. Tiwari, Phys.Rev. **D86**, 125016 (2012)
 - [22] D. J. Gross, R. D. Pisarski, and L. G. Yaffe, Rev. Mod. Phys. **53**, 43 (1981).
 - [23] L. D. McLerran and B. Svetitsky, Phys. Rev. **D24**, 450 (1981).
 - [24] G. Boyd et al., Nucl. Phys. **B469**, 419 (1996).
 - [25] M. Okamoto et al. (CP-PACS), Phys. Rev. **D60**, 094510 (1999)
 - [26] K. Fukushima, Phys.Lett. **B591**, 277 (2004)
 - [27] A. Dumitru, D. Roder, and J. Ruppert, Phys.Rev. **D70**, 074001 (2004)
 - [28] V. Dixit and M. C. Ogilvie, Phys.Lett. **B269**, 353 (1991).
 - [29] S. Phatak, Phys.Rev. **C58**, 2383 (1998)
 - [30] T. M. Kalotas and A. R. Lee, Am. J. Phys. **59**, 48 (1991).